HHS Public Access

Author manuscript

*Mol Pharm*. Author manuscript; available in PMC 2017 June 06.

Published in final edited form as:

*Mol Pharm*. 2016 June 6; 13(6): 2026–2038. doi:10.1021/acs.molpharmaceut.6b00159.

# Development of $GABA_A$ Receptor Subtype-Selective Imidazobenzodiazepines as Novel Asthma Treatments

**Gloria S. Forkuo**[1], **Margaret L. Guthrie**[1], **Nina Y. Yuan**[1], **Amanda N. Nieman**[1], **Revathi Kodali**[1], **Rajwana Jahan**[1], **Michael R. Stephen**[1], **Gene T. Yocum**[2], **Marco Treven**[3], **Michael M. Poe**[1], **Guanguan Li**[1], **Olivia B. Yu**[1], **Benjamin D. Hartzler**[1], **Nicolas M. Zahn**[1], **Margot Ernst**[3], **Charles W. Emala**[2], **Douglas C. Stafford**[1], **James M. Cook**[1], and **Leggy A. Arnold**[1,*]

[1]Department of Chemistry and Biochemistry and the Milwaukee Institute for Drug Discovery, University of Wisconsin-Milwaukee, Milwaukee, Wisconsin, 53201

[2]Department of Anesthesiology, Columbia University, New York, New York, 10032

[3]Department of Molecular Neurosciences, Medical University of Vienna, Vienna, Austria

## Abstract

Recent studies have demonstrated that subtype-selective $GABA_A$ receptor modulators are able to relax pre-contracted human airway smooth muscle *ex vivo* and reduce airway hyper-responsiveness in mice upon aerosol administration. Our goal in this study was to investigate systemic administration of subtype-selective $GABA_A$ receptor modulators to alleviate bronchoconstriction in a mouse model of asthma. Expression of $GABA_A$ receptor subunits was identified in mouse lungs and the effects of α4-subunit-selective $GABA_AR$ modulators, XHE-III-74EE and its metabolite XHE-III-74A, were investigated in a murine model of asthma (ovalbumin sensitized and challenged BALB/c mice). We observed that chronic treatment with XHE-III-74EE significantly reduced airway hyper-responsiveness. In addition, acute treatment with XHE-III-74A but not XHE-III-74EE decreased airway eosinophilia. Immune suppressive activity was also shown in activated human T-cells with a reduction in IL-2 expression and intracellular calcium concentrations $[Ca^{2+}]_i$ in the presence of GABA or XHE-III-74A, whereas XHE-III-74EE showed only partial reduction of $[Ca^{2+}]_i$ and no inhibition of IL-2 secretion. However, both compounds significantly relaxed pre-contracted tracheal rings *ex vivo*. Overall, we conclude that the systemic delivery of a α4-subunit-selective $GABA_AR$ modulator shows good potential for a novel asthma therapy, however, the pharmacokinetic properties of this class of drug candidates have to be improved to enable better beneficial systemic pharmacodynamic effects.

*Corresponding Author: Leggy A. Arnold, Department of Chemistry and Biochemistry, University of Wisconsin-Milwaukee, Milwaukee, Wisconsin, 53201, arnold2@uwm.edu.

Supporting Information. The supporting information contain the detail description and analysis of XHE-III-74EE and XHE-III-74A, their microsomal stability and pharmacokinetic profile. This material is available free of charge via the Internet at http://pubs.acs.org.

**Author Contributions**: The manuscript was written through contributions of all authors. All authors have given approval to the final version of the manuscript.

**Keywords**

Asthma; GABA; $GABA_A$ receptor; airway smooth muscle; inflammation; eosinophilia; XHE-III-74EE; XHE-III-74A

## Introduction

Asthma is a chronic inflammatory disease of the airways, which in the United States affects over 39.5 million people including 8.7 million children.[1] The disease is characterized by three major features: inflammation, mucous production, and airway hyper-responsiveness.[2] The mainstays of asthma management include anti-inflammatory agents, including inhaled corticosteroids used alone or in combination with potent bronchodilators, such as $\beta_2$ adrenoceptor agonists. The disease may become resistant to these traditional therapies and the chronic use of these medications is associated with adverse side effects,[3-6] thus new therapeutics are needed to manage this major public health problem.

The $GABA_A$ family of receptors ($GABA_AR$), which are well-established drug targets for central nervous system disorders, are a promising new pharmacological target to alleviate asthma symptoms. Importantly, $GABA_AR$ have been shown to mediate immune-modulatory effects and airway smooth muscle (ASM) relaxation in the lung.[7-9] $GABA_AR$ are heteropentameric ligand-gated chloride channels consisting of combinations of 19 different subunits ($\alpha_{1-6}$, $\beta_{1-3}$, $\gamma_{1-3}$, $\delta$, $\varepsilon$, $\pi$, $\theta$, $\rho_{1-3}$). In the central nervous system the receptors classically consist of two $\alpha$, two $\beta$ and a third subunit ($\gamma$ and $\delta$).[10, 11] The subunit compositions of the receptors impact ligand selectivity, which has led to the development of subtype selective drugs with restricted pharmacological effects, kinetics, and regional CNS effects.[12-14] For example, brain $GABA_AR$ containing $\alpha1$, $\alpha2$ or $\alpha3$ subunits can be targeted selectively by positive modulators to induce sedation ($\alpha1$) or reduce anxiety ($\alpha2/\alpha3$).[15-17]

In the mammalian airway, ASM expresses $GABA_AR$ containing $\alpha4$ and $\alpha5$ subunits,[8] and both $\alpha4$ and $\alpha5$ selective $GABA_AR$ positive modulators were able to relax pre-contracted ASM.[18-20] In addition, $GABA_AR$, including those with $\alpha4$ subunits, are found in the membrane of various immune cells.[21-23] GABA (the natural ligand of the $GABA_AR$) and muscimol (a full $GABA_AR$ agonist) elicited significant lymphocyte membrane currents and GABA decreased phytohemagglutinin-induced T-cell proliferation; consistent with our proposed model that activation (by GABA) of depolarizing $Cl^-$ channels decreases $Ca^{2+}$ entry into lymphocytes, thus reducing $Ca^{2+}$ dependent lymphocyte activation signaling. GABA also reduced cytokine secretion (IL-6 and IL-12) in LPS-stimulated peritoneal macrophages.[24] Importantly, in acute and chronic mouse models it has been shown that honokiol, a naturally occurring non-selective positive allosteric $GABA_AR$ modulator, not only decreased the levels of IL-6 and IL-12 in spleen cells, but also IL-2, IL-7, IL-17, TNF$\alpha$ and IFN$\gamma$.[25] However, the efficacy of chronic treatment with alpha subtype-selective $GABA_AR$ modulators in asthmatic mouse models has not been reported. In asthma, the epithelium undergoes remodeling characterized by goblet cell hyperplasia and mucus hypersecretion. In ovalbumin sensitized and challenged (asthmatic) mice, non-selective GABA antagonist bicuculline and channel blocker picrotoxin reduced mucus overproduction

and decreased GABA-induced depolarization of human airway epithelia cells, but did not alter the airway hyper-responsiveness of methacholine-challenged mice.[26]

Taken together, the GABAergic system represents a compelling new drug target for asthma in light of its influence on ASM relaxation, inflammatory modulation, and regulation of mucus hypersecretion. Here, we report the initial pharmacological evaluation of α4-subtype selective $GABA_AR$ modulators, XHE-III-74 ethyl ester (XHE-III-74EE or L-655,708)[27] and its metabolite XHE-III-74 acid (XHE-III-74A) as potential drug leads for asthma.

## Experimental Section

Chemicals: XHE-III-74EE and XHE-III-74A were synthesized using a published procedure. 28 The purity of both compounds (>98%) was confirmed by NMR and HPLC. (see supporting information).

### Experimental animals

5-10 weeks old male BALB/c and Swiss Webster mice (Charles River Laboratory, WIL, MA) were used for the experiments. Mice were housed under specific pathogen-free conditions, under standard conditions of humidity, temperature and a controlled 12 h light and dark cycle and had free access to food and water. All animal experiments were in compliance with the University of Wisconsin, Milwaukee Institutional Animal Care and Use Committee (IACUC). Airway smooth muscle in tracheal rings were obtained from guinea pigs (male 400 g Dunkin-Hartley) in accordance with approval from the Columbia University IACUC.

### Immunoblot analysis

Whole lungs from control and Ova S/C BALB/c mice were lysed, combined with a protease inhibitor cocktail tablet (Roche Applied Sciences, Indianapolis, IN), and membrane protein was extracted using the Mem-PER™ Plus membrane protein extraction kit (following manufacturer's instructions, Thermo Fisher Scientific Inc., Rockford, IL). The membrane protein concentration was determined by the Pierce™ Coomassie (Bradford) protein assay kit (Thermo Fisher Scientific Inc., Rockford, IL), according to the manufacturer's instructions. Protein extracts were subjected to SDS-PAGE using NuPAGE Novex 4-12% Bis-Tris protein gels (Thermo Fisher Scientific Inc, Rockford, IL) and transblotted onto nitrocellulose iBlot® 2 transfer stacks (Thermo Fisher Scientific Inc, Rockford, IL) using the iBlot® 2 gel transfer device. Membranes were blocked in superblock™ T20 (TBS) blocking buffer (Thermo Fisher Scientific Inc., Rockford, IL) for 1 hour at room temperature and then incubated with primary antibodies (α1 (sc-7348), α2 (MABN1724), α3 (sc-133603), α4 (sc-7355), α5 (sc-31417), β3 (sc-376252), and γ2 (sc-101963) overnight at 4°C. This was followed by treatment for 1 hour with HRP conjugated secondary antibodies and protein bands were developed using Pierce™ ECL western blotting substrate (Thermo Fisher Scientific Inc, Rockford, IL) according to manufacturer's recommendations. A CCD camera connected to FluorChem HD2/FC2 (Cell Biosciences Inc, Santa Clara, CA) was used to capture the digital images.

### Immunohistochemistry

Formalin fixed and paraffin embedded lungs were sectioned and rehydrated. Heat-mediated antigen retrieval was done with 10 mM sodium citrate buffer, pH = 6 (Sigma-Aldrich, St. Louis, MO) for 10 minutes. This was followed by endogenous peroxidase suppression for 15 minutes with the peroxidase suppressor (Thermo Fisher Scientific Inc, Rockford, IL) and non-specific protein blockade with the background sniper (Thermo Fisher Scientific Inc, Rockford, IL) for 10 minutes. Slides were incubated overnight at 4°C in primary antibodies against the α4 $GABA_A$ receptor subunit (goat polyclonal, 1:200; Santa Cruz Biotechnology, CA, sc-7355) in superblock™ T20 (TBS) blocking buffer (Thermo Fisher Scientific Inc., Rockford, IL). After overnight incubation, slides were washed three times with TBST (Thermo Fisher Scientific Inc., Rockford, IL) followed by secondary antibody (donkey anti-goat, 1:50; Santa Cruz Biotechnology, CA, sc-2033) incubation at room temperature for 40 minutes. A parallel lung section was incubated in secondary antibody as negative control. The antigen antibody complex was then visualized with the peroxidase substrate kit, DAB substrate kit (Thermo Fisher Scientific Inc., Rockford, IL). Sections were counterstained with hematoxylin (Sigma-Aldrich, St. Louis, MO), dried, dehydrated in graded alcohol series and histoclear, and cover slipped using Permount™ mounting media (Fisher Scientific, Pittsburgh, PA).

### Microsomal stability and pharmacokinetic study (see supplementary information)

**Cell culture Jurkat—**Jurkat cells were maintained in suspension in RPMI 1640 medium with L-glutamine (Thermo Fisher Scientific Inc., Rockford, IL) supplemented with 10% (v/v) fetal bovine serum. The cells were maintained in 5% $CO_2$, 95% humidified air at 37°C at an approximate density of $10^6$ cells/ml.

**Electrophysiological experiments with Xenopus oocytes have been reported—**[25, 26] Mature female Xenopus laevis (Nasco, Fort Atkinson, WI, USA) were anaesthetized in a bath of ice-cold 0.17% Tricain (Ethyl-m-aminobenzoat, Sigma-Aldrich, St. Louis, MO, USA) before decapitation and transfer of the frog's ovary to ND96 medium (96 mM NaCl, 2 mM KCl, 1 mM $MgCl_2$, 5 mM HEPES; pH 7.5). Following incubation in 1mg/ml collagenase (Sigma-Aldrich, St. Louis, MO, USA) for 30 min, stage 5 to 6 oocytes were singled out of the ovary and defolliculated using a platinum wire loop. Oocytes were stored and incubated at 18°C in NDE medium (96 mM NaCl, 2 mM KCl, 1 mM $MgCl_2$, 5 mM HEPES, 1.8 mM $CaCl_2$; pH 7.5) that was supplemented with 100 $U \cdot mL^{-1}$ penicillin, 100 $\mu g \cdot mL^{-1}$ streptomycin and 2.5 mM pyruvate. Oocytes were injected with an aqueous solution of mRNA. A total of 2.5 ng of mRNA per oocyte was injected. Subunit ratio was 1:1:5 for αxβ3γ2 (x = 1,2,3,5) and 3:1:5 for α4β3γ2 receptors. Injected oocytes were incubated for at least 36 h before electrophysiological recordings. Oocytes were placed on a nylon-grid in a bath of NDE medium. For current measurements, the oocytes were impaled with two microelectrodes (2–3MΩ), which were filled with 2M KCl. The oocytes were constantly washed by a flow of 6 $mL \cdot min^{-1}$ NDE that could be switched to NDE containing GABA and/or drugs. Drugs were diluted into NDE from DMSO solutions resulting in a final concentration of 0.1% DMSO. Maximum currents measured in mRNA injected oocytes were in the microampere range for all receptor subtypes. To test for modulation of GABA induced currents by compounds, a GABA concentration that was titrated to trigger 3-5% of

the respective maximum GABA-elicited current of the individual oocyte (EC3-5) was applied to the cell together with various concentrations of tested compounds. All recordings were performed at room temperature at a holding potential of -60 mV using a Warner OC-725C TEV (Warner Instrument, Hamden, CT, USA) or a Dagan CA-1B Oocyte Clamp or a Dagan TEV-200A TEV (Dagan Corporation, Mineapolis, MN, USA). Data were digitized using a Digidata 1322A or 1550 data acquisition system (Axon Instruments, Union City, CA, USA), recorded using Clampex 10.5 software (Molecular Devices, Sunnyvale, CA, USA), and analyzed using Clampfit 10.5 and GraphPad Prism 6.0 (La Jolla, CA, USA) software. Concentration-response data were fitted using the Hill equation. Data are given as mean ± SEM from at least three oocytes of two batches.

**Rotarod assay—**BALB/c mice were trained to maintain balance at a constant speed of 15 rpm on the rotarod apparatus (Omnitech Electronics Inc., Nova Scotia, Canada) until mice could perform for three minutes at three consecutive time points. Separate groups of mice received intraperitoneal (i.p.) injections of vehicle (10% DMSO, 40% propylene glycol and 50% PBS), test compounds (XHE-III-74 ethyl ester (1, 5, 20 or 40 mg/kg) or XHE-III-74 acid (1, 5, 20 mg/kg), and diazepam as a positive control compound (1 mg/kg or 5 mg/kg) in an approximate volume of 100 μl. Five to ten minutes after each injection, mice were placed on the rotarod for three minutes. A fail was assigned for each mouse that fell from the rotarod prior to 3 minutes. Mice were rested two to three days before administration of another dose or a different compound. The protocol was changed to a 200 μl i.p. injection for vehicle and 40 mg/kg XHE-III-74 ethyl ester due to solubility.

**Ovalbumin sensitization and challenge and drug treatment protocol—**Randomized male Balb/c mice were sensitized three times with i.p. injections of 2 mg/kg/d ovalbumin (Ova) (Sigma-Aldrich, St. Louis, MO) emulsified in 2 mg of Alum (Imject Alum; Thermo Scientific, Pierce, Rockford, IL) on days 0, 7 and 14 in a total volume of 100 μL. Mice were then challenged intra-nasally (i.n.) with 1 mg/kg/d Ova for 5 days from days 23–27. Control mice were sensitized with Ova and challenged with saline.[29] The acute and repeated dosing effects of XHE-III 74A and XHE-III 74EE were tested in separate groups of Ova sensitized and challenged (Ova S/C) Balb/c mice. For acute drug treatment, mice received a single i.p. injection of either XHE-III-74A or XHE-III-74EE for 40 minutes before assessment of airway parameters. For repeated dosing drug treatments, mice received two i.p. injections of either XHE-III-74A or XHE-III-74EE for five days during the Ova challenge period. Alternatively, groups of Ova S/C Balb/c mice were surgically implanted with osmotic minipumps (Alzet®, 1007D pumps) to release XHE-III-74EE at a dose of 20 mg/kg/day for 7 days. Airway parameters were assessed on day 28.

**Assessment of Airway hyper-responsiveness—**Airway hyper-responsiveness to methacholine in conscious, spontaneously breathing animals was measured by DSI's Buxco® FinePointe Non-Invasive Airway Mechanics (NAM) instrument.[30] Before measurements were taken, mice were acclimated to the chambers 15 minutes daily for 5 days. The chambers were also calibrated each time before data collection. Briefly, the nasal chamber in combination with the thoracic chamber allows computation of Specific Airway Resistance (sRaw). The FinePointe software computes sRaw with all other ventilatory

parameters derived by the NAM analyzer. Mice were exposed to aerosolized PBS (for the baseline measurement) or methacholine (1.56-12.5 mg/ml) for 1 minute and readings were taken and averaged for 3 minutes after each nebulization. Data obtained were presented as sRaw versus aerosolized methacholine concentration (mg/ml).

**Histopathological analysis of lung sections—**After determination of AHR and BALF collection, the lungs of mice were perfused with 10% neutral buffered cold formalin (Sigma-Aldrich, St. Louis, MO) through the tracheal cannula. Following lung perfusion, the trachea was tied with a suture to avoid leakage of the formalin and to ensure the lungs are well fixed. Lungs were then isolated from the thoracic cavity and kept in 10% neutral buffered cold formalin for 48 hours at 4°C. The left lobe was then sectioned transversely into two. Sample dehydration, paraffin embedding and sectioning was performed by CRI Histology Research Core Facility (Milwaukee, WI). 5 μm microtome sections were placed on positively charged slides, dewaxed with histoclear, and rehydrated in graded concentrations of ethanol. Following rehydration, sections were oxidized in 1% periodic acid and incubated in fluorescent Schiff's reagent for 20 minutes at room temperature. Slides were washed with distilled water, rinsed in acid alcohol, and cover slipped with Canada balsam and methyl salicylate mounting media to obtain Periodic Acid Fluorescent Schiff's (PAFS) stained slides.[31, 32] The PAFS-stained slides were examined under the EVOS fluorescence microscope and images from random fields acquired from the axial bronchi. Image J software was used to obtain mucin volume density by morphometrically determining the area of mucin glycoprotein in the epithelium per length of the basement membrane.[31, 32] Scale bars obtained during image acquisition were used to scale the images.

**Eosinophil count—**Mice were euthanized with a cocktail of ketamine (300 mg/kg) and xylazine (30 mg/kg) (Sigma Aldrich, St. Louis, MO) in an approximate volume of 100 μL per i.p. injection. The lungs were dissected and tracheotomized with an 18G luer stub adapter. The left lung was clamped using a hemostat and the right lung perfused with 500 μL sterile saline. Broncho-alveolar lavage fluid was then pooled and aspirated into tubes and spun unto positively charged slides using Thermo Shandon Cytopsin® 3 (Marshal Scientific, Brentwood, NH). Slides were stained with Wright Giemsa stain (Sigma-Aldrich, St. Louis, MO) and washed with $ddH_20$ for 10 minutes. The slides were cover slipped with Permount™ mounting media (Fisher Scientific, Pittsburgh, PA) and eosinophils counted in four randomly chosen 20× light microscope fields, and expressed as percentage of total cells.[29, 33]

**IL-2 ELISA assay—**Jurkat cells were collected, pelleted, and resuspended in media at a final concentration of 400,000 cells/mL and dispensed at 10,000 cells/well (200 μl/well) into a 96 well plate. 200 nl of test compound in DMSO or GABA (Sigma-Aldrich, St. Louis, MO) in water was added with the TECAN automated liquid handling robot system. After 15 minutes, 10 μl of a mixture of 25 μg/mL phytohemagglutinin (Fisher Scientific, Pittsburgh, PA) and 1.25 μg/ml phorbol myristate acetate (Fisher Scientific, Pittsburgh, PA) in PBS:DMSO (80:1) were added followed by incubation for 24 hours at 37°C. The plate was centrifuged at 1000 rpm for 3 minutes and 100 μl of supernatant analyzed using a BD

Human IL-2 ELISA kit II (Fisher Scientific, Pittsburgh, PA) following the manufacturer's instructions.

**Intracellular Calcium assay—**The Fluo-4 NW calcium assay kit (Life Technologies, Rockford, IL) was used for intracellular calcium measurements. Briefly, Jurkat cells were collected, pelleted, and resuspended in Fluo-4 NW assay buffer at a final concentration of $5\times10^6$ cells/ml and dispensed at 125,000 cells/well (25 μl/well) into a 384 NUNC white optical bottom well plate (Fisher Scientific, Pittsburgh, PA). It was then centrifuged at 1000 rpm for 3 minutes, and incubated at 37°C for one hour. 25 μl of 2× Fluo-4 NW dye was added to each well followed by incubation for 30 minutes at 37°C and 15 minutes at room temperature. 1 μl of test compound in DMSO or GABA in water was added to each well and incubated for 15 minutes at room temperature. Activation was induced with 2 μl of a mixture of 25 μg/mL phytohemagglutinin and 1.25 μg/ml phorbol myristate acetate in PBS: DMSO (80:1) Fluorescence intensity was recorded every 10 seconds for a total of 300 seconds using a TECAN M1000 plate reader (TECAN, Maennedorf, Switzerland) at an excitation and emission spectra of 494 nm and 516 nm, respectively.

**Automated patch-clamp electrophysiology for Jurkat cells—**The IonFlux plate layout consists of units of twelve wells; two wells contain intracellular solution (ICS containing 140 mM CsCl 1 mM $CaCl_2$, 1 mM $MgCl_2$, 11 mM EGTA, 10 mM HEPES, pH 7.2 with CsOH), one contains cells diluted in extracellular solution (ECS containing 140 mM NaCl, 5 mM KCl, 2 mM $CaCl_2$, 1 mM $MgCl_2$, 5 mM D-glucose monohydrate, and 10 mM HEPES, pH 7.4 with NaOH), eight contain the compounds of interest diluted in ECS, and one well is for waste collection. Cells are captured from suspension by applying suction to microscopic channels in ensemble recording arrays. Once the array is fully occupied, the applied suction breaks the cell membranes of captured cells, establishing whole cell voltage clamp. For compound applications, pressure is applied to the appropriate compound wells, introducing the compound into the extracellular solution rapidly flowing over the cells. For recording $GABA_A$ currents, cell arrays were voltage clamped at a hyperpolarizing holding potential of -80 mV. Prior to use on the automated patch clamp, cells were centrifuged at 380 × g for 5 minutes and gently resuspended in ECS. This was repeated two more times before dispensing the cells into the plate. 10 mM stock solutions of XHE-III-74A and XHE-III-EE in DMSO were diluted to appropriate concentrations in ECS and co-applied with 0.3 μM GABA.

**Guinea Pig Airway Smooth Muscle Organ Bath Experiments—**Adult male Hartley guinea pigs were deeply anesthetized by intraperitoneal pentobarbital (100 mg/kg). The tracheas were surgically removed and transected into cross sections containing 2 cartilaginous rings. After removing the epithelium with a cotton swab, the rings were suspended from 2 silk threads in a 4-ml jacketed organ bath (Radnoti Glass Technology), with one thread attached to a Grass FT03 force transducer (Grass-Telefactor) coupled to a computer via Biopac hardware and Acknowledge 7.3.3 software (Biopac Systems) for continuous digital recording of muscle tension. The rings were bathed in 4 ml of KH buffer solution (composition in mM: 118 NaCl, 5.6 KCl, 0.5 $CaCl_2$, 0.2 $MgSO_4$, 25 $NaHCO_3$, 1.3 $NaH_2PO_4$, 5.6 D-glucose) with 10 μM indomethacin (DMSO vehicle final concentration of

0.01%), which was continuously bubbled with 95% $O_2$ and 5% $CO_2$ at pH 7.4, 37°C. The rings were equilibrated at 1 g of isotonic tension for 1 h with new KH buffer added every 15 min. All rings were precontracted with 10 μM N-vanillylnonanamide (capsaicin analog) and then 2 cycles of cumulatively increasing concentrations of acetylcholine (0.1–100 μM) with extensive buffer washes between and after those 2 cycles with resetting of the resting tension to 1.0 g. Tetrodotoxin (1 μM) and pyrilamine (10 μM) were added to the buffer in the baths to eliminate the confounding effects of airway nerves and histamine receptors. After a stable baseline at 1.0g resting tension was established, tracheal rings were contracted with 1 μM of substance P. After the peak contraction was reached, 100 μM XHE-III-74, XHE-III-74EE, XHE-III-74A or vehicle (0.1% DMSO) was added to the bath. The percentage of initial contraction remaining 30 minutes after compound exposure was compared between groups.

**Statistical analysis—**Results of experiments were graphed using GraphPad Prism 4 (GraphPad Software, San Diego, CA) and data are expressed as mean ±SEM. One-way analysis of variance (ANOVA) with Dunnet post-hoc test or two-way ANOVA with Bonferroni post-hoc test were performed for statistical difference for multiple groups. For comparison of two groups, a two-tailed unpaired Student's t test was used. Statistical significance was defined as $p<0.05$ using GraphPad Prism 4.

## Results

We have investigated the pharmacological effects of α4-selective $GABA_AR$ positive modulators in an ovalbumin sensitized and challenged (Ova S/C) murine model of asthma that represents an acute allergic pulmonary inflammation model.[34] Immunoblot and immunohistochemistry analyses were used to identify $GABA_AR$ subunits in the mouse lung (Figure 1).

In agreement with published results, α1 and α2 proteins were observed as immunoreactive bands at the appropriate weight of 52 kDa and 53 kDa (Figure 1, A-C).[35] However, in contrast to mouse brain, no α3 $GABA_AR$ subunits were detected in mouse lungs. Similarly, α1 subunit mRNA was detected at significant levels in adult rat lung[36] and the α2 subunit protein detected in mouse lung.[36] However, cell-specific $GABA_AR$ subunit expression in carefully dissected airway smooth muscle from human and guinea pig trachea showed the α4 and α5 mRNA transcripts were the only α $GABA_AR$ subunits detected.[8] In addition, a band at 65 kDa was observed for α2 $GABA_AR$ subunit that was comparable to the immuoreactive band from mouse cerebellum extract (Figure 1, B). For the α4 subunit, we observed a weak immunoreactive band with the molecular weight of 55 kDa that was comparable to the protein band observed for the neuroglioma cell lysate (H4) control (Figure 1, D). Jurkat cells also expressed the α4 $GABA_AR$ subunit with the same molecular weight (Figure 1, H). The α5 $GABA_AR$ subunit was visualized as an immunoreactive band at 65 kDa, similar to the mouse brain extract control (Figure 1 E). We also identified β3 and γ2 subunits, which are common subunits in the $GABA_AR$ (Figure 1, F and G). An immunoreactive band at the expected molecular weight of 52 kDa was identified for the γ2 subunit and at 55 kDa for the β3 subunit.[37] To assess the localization of the α4 $GABA_AR$ subunit in different areas of the lungs, we performed immunohistochemistry analysis. Positive staining of the α4 subunits was observed in the airway epithelium, smooth muscle

and chondrocytes (Figure 1, J and K). Differentiated epithelial cells in our Ova S/C Balb/c mouse lungs expressed the α4 subunit as well (Figure 1, K).

We reported previously that α4/α6 selective $GABA_AR$ positive modulators XHE-III-74 and CMD-45 (Figure 2) were able to relax pre-contracted ASM *ex vivo* and in addition, XHE-III-74 reduced ASM *in vivo* lung resistance in a house dust mite mouse model of asthma when given as an aerosol.[18, 20]

Encouraged by these results, we evaluated the metabolic stability of XHE-III-74 before investigating repeated dosing of α4 selective $GABA_AR$ positive modulators to reduce methacholine-induced resistance in mouse lungs. Table 1 shows the percent of XHE-III-74 remaining following incubation with human and mouse liver microsomes for 1 hour.

XHE-III-74, although stable in human liver microsomes, was metabolized rapidly by mouse liver microsomes, with 24.1% remaining after 1 hour - corresponding to a half-life of less than 24 minutes. To overcome any species-dependent stability differences of XHE-III-74, analogs of this compound were synthesized leading to XHE-III-74 ethyl ester (XHE-III-74EE), which was shown to be stable in both human and mouse liver microsomes, as well as the respective S9 liver fractions, for an hour with a predicted half-life of several hours (Table 1).

Mass analysis of XHE-III-74EE metabolism revealed hydrolysis of the ester moiety to its corresponding carboxylic acid, resulting in XHE-III-74A (data not shown). This prompted us to synthesize and evaluate the stability of XHE-III-74A in the presence of mouse and human liver microsomes and corresponding S9 fractions. As with the parent molecule, we did not observe species-specific metabolism for XHE-III-74A, although XHE-III-74A was more rapidly metabolized than XHE-III-74EE, with a remaining percentage after one hour for human and mouse liver microsomes of 56.5 ± 0.6% and 51.3 ±0.4%, respectively (Table 1). The half-lives for human and mouse liver microsomes were 80.1 ± 10.1 minutes and 73.4 ± 6.5 minutes, respectively (Supporting Information). We observed a similar metabolic stability for both compounds in S9 fractions. Both compounds were stable in the presence of blood plasma for at least one hour.

To extend the *in vitro* metabolism studies and to confirm compound stability *in vivo*, a single dose pharmacokinetic study was performed in mice. Animals were administered 5 mg/kg of XHE-III-74EE in a single i.p injection in vehicle (10% DMSO, 40% propylene glycol and 50% PBS). (Figure 3, A).

The absorption and distribution of XHE-III-74EE in blood and lung was rapid with a $T_{max}$ of 10 and 3 minutes, respectively. The $C_{max}$ was roughly two times higher in blood than in lung and the AUC of XHE-III-74EE in lung was 60% of the blood AUC. These data confirm good distribution of XHE-III-74EE in the target organ for potential asthma therapy (lungs). However, the half-life of XHE-III-74EE in lung was only 17.6 minutes. In addition, the AUC of XHE-III-74EE in brain is 79% of the AUC in blood, thus XHE-III-74EE is able to penetrate the blood-brain barrier (BBB) and has a relatively long brain half-life (36.7 minutes). To distinguish between clearance and metabolism of XHE-III-74EE in blood, lung and brain, we quantified the amount of metabolic product XHE-III-74A for the animals

treated with XHE-III-74EE (Figure 3, B). Interestingly, only blood contained quantifiable amounts of XHE-III-74A. The AUC of XHE-III-74A in blood was 75% of the AUC of XHE-III-74EE indicating that the rate of metabolism of XHE-III-74EE to XHE-III-74A in blood is significantly faster than its rate of clearance. However, XHE-III-74EE is stable in blood plasma, thus metabolism is likely to occur in the liver. The presence of XHE-III-74EE in brain and lung and absence of XHE-III-74A indicates that these organs do not support metabolism of XHE-III-74EE into XHE-III-74A. The pharmacokinetic analysis of XHE-III-74A similarly given at 5 mg/kg showed a rapid absorption and distribution similar to XHE-III-74EE, with a $T_{max}$ of 10 minutes for lung and blood (Figure 3, C). The AUC of lung and blood were comparable indicating excellent distribution of XHE-III-74A in lung tissue. However, as indicated above, XHE-III-74A is cleared rapidly from lung and blood with half-lives of 11.0 and 13.1 minutes, respectively. In contrast to XHE-III-74EE, the concentration of XHE-III-74A in the brain was very low; indicating poor penetration of XHE-III-74A across the BBB. The quantification of XHE-III-74A at the 30 minute pharmacokinetic time point confirmed the low concentration of XHE-III-74A in brain and identified very high levels of XHE-III-74A in urine (Figure 3, D). The concentration of XHE-III-74A was also significant in the kidneys supporting the hypothesis that most of XHE-III-74A is excreted unchanged. However, the concentration of XHE-III-74A in liver (4% of the concentration in blood) was significantly lower than in all other organs making it possibly the main site of metabolism.

XHE-III-74EE has been reported as α4β3γ2 subtype-selective $GABA_AR$ modulator with some activity at the α6β3γ2 $GABA_AR$ at concentrations higher that 1 μM.27 Herein, we show the evaluation of XHE-III-74A in oocytes individually expressing single α (α 1-5) subunits of GABAAR in combination with β3 and γ2 subunits (Figure 4), in direct comparison with XHE-III-74EE.

Using two electrode voltage clamp current recordings in the presence of a concentration of GABA that elicited 3-5% of the maximal GABA induced current ($EC_{3-5}$), increasing concentrations of the acid metabolite, XHE-III-74A, exhibited modulatory effects only in the α4β3γ2 and α5β3γ2 $GABA_ARs$, while being largely inactive in the α1β3γ2, α2β3γ2 and α3β3γ2 subtypes. At 30 μM and above, XHE-III-74A had selectivity biased to the α4β3γ2 receptor, while reaching a plateau at α5β3γ2 receptors.

To evaluate possible CNS effects caused by XHE-III-74EE due to its ability to penetrate the BBB, a motor sensory study was carried out using the rotarod method (Figure 5).

Male Balb/c mice were injected i.p. with the indicated compound and after 10 minutes evaluated for the ability to stay afoot on a rotating rod moving at 15 rpm. In this test diazepam, a classical alpha subunit non-selective $GABA_AR$ positive modulator that binds to the α1β3γ2 $GABA_AR$,[17] induced significant motor impairment at 5 mg/kg. At the same concentration, XHE-III-74EE did not impair motorsensory coordination. Escalating dosages to 40 mg/kg did cause motor-impairing effects. In contrast, XHE-III-74A was devoid of motor effects at 20 mg/kg, consistent with the inability of XHE-III-74A to penetrate the BBB.

Based on these results, compounds were evaluated in an Ova sensitized mouse asthma model.[34] In this model, airway inflammation is established in Balb/c mice by Ova given first i.p. followed by intra-nasal challenge, which results in airway hyperresponsiveness (AHR), mucus hypersecretion, and inflammation. Primed mice were administered XHE-III-74EE or XHE-III-74A i.p. during the Ova challenge phase (chronic repeated dosing) or 40 minutes (acute) before AHR measurement using DSI's Buxco® FinePointe non-invasive airway mechanics instrument (Figure 6).

Asthmatic mice treated twice daily for 5 days with 20 mg/kg of XHE-III-74EE exhibited reduced methacholine-induced AHR (caused a downward shift in sRaw) (Figure 6A). In contrast, single i.p. administration of XHE-III-74EE at 10 or 20 mg/kg did not alter AHR (Figure 6, B and C). Taking into account the fast metabolism of XHE-III-74EE and rapid clearance of XHE-III-74A, we used surgically implanted minipumps that released XHE-III-74EE continuously over a period of seven days, resulting in a constant blood concentration of XHE-III-74EE of 27.2 ± 2.7 ng/g at the day of AHR measurement. Pump delivery of XHE-III-74EE was effective in reducing AHR at low concentrations of methacholine, whereas concentrations of 6.25 mg/mL and higher did not result in a significant improvement from untreated control mice (Figure 6, D and B). A similar trend was observed with the well-known anti-inflammatory agent dexamethasone, which was used as positive control in our model (Figure 6E). Because the animals are not sedated during the measurement, conscious changes of breathing can influence results at severe bronchoconstriction. Notably, we observed that at methacholine concentrations higher than 12.5 mg/mL mice tended to hold their breath to minimize unpleasant bronchoconstriction. Finally, acute administration of XHE-III-74A (20 mg/kg i.p. 40 minutes prior to airway measurements) did not result in a significant reduction in methacholine-induced AHR (Figure 6F).

Lung sections from treated and untreated OVA mice were stained with periodic acid fluorescent Schiff's (PAFS) stain to evaluate mucus hypersecretion (Figure 7).

Ova S/C mice exhibited a significant increase of mucus in their large bronchioles. A single i.p. injection of dexamethasone daily for 8 days (4 mg/kg) significantly decreased mucous metaplasia in Ova S/C mice compared to the vehicle treated mice ($p<0.01$). Treatment with XHE-III-74EE or XHE-III-74A (20 mg/kg i.p. injections daily for 5 days) did not significantly change airway mucous metaplasia in comparison to vehicle treated Ova S/C mice. In addition, there was no change in airway mucous metaplasia with continuous administration of 20 mg/kg/day XHE-III-74EE via osmotic pump implantation. Finally, the acute treatment of XHE-III-74EE and XHE-III-74A (single i.p. injection for 40 minutes) did not change mucin production.

In addition, we quantified the immune response in the lungs of Ova S/C mice by collecting the bronchoalveolar lavage fluid (BALF) followed by the quantification of eosinophils using a Wright Giemsa stain (Figure 8).

The Ova asthma model demonstrates mainly eosinophil-driven lung inflammation.[34] As reported, dexamethasone treatment in Ova S/C mice significantly decreased airway

eosinophilia compared to vehicle-treated mice (Figure 8).[38] However, acute (single i.p. injection for 40 minutes) and repeated dosing (twice i.p. injection for 5 days) administration of 20 mg/kg XHE-III-74EE to Ova S/C mice were not effective in reducing airway eosinophilia. In addition, there was no change in airway eosinophilia with repeated dosing administration of 20 mg/kg XHE-III-74EE via osmotic pump implantation. However, we observed a significant decrease in airway eosinophilia compared to the vehicle-treated mice following the acute treatment of Ova S/C mice with 20 mg/kg XHE-III-74A for 40 minutes ($p<0.05$). Although XHE-III-74A is a metabolite of XHE-III-74EE, we did not observe a similar beneficial decrease in eosinophils with acute administration of XHE-III-74EE. This can be accounted for by the fact that XHE-III-74EE is metabolized into XHE-III-74A in the blood but not in the lungs. The repeated dosing of two injections daily of 20 mg/kg XHE-III-74A acid for 5 days, however, was not effective at reducing BALF eosinophilia.

To investigate the direct influence of XHE-III-74EE and its metabolic product XHE-III-74A on immune cells, we investigated effects on human Jurkat T-cells in vitro (Figure 9). When stimulated with phytohemagglutinin (PHA) and phorbol myristate acetate (PMA), cell activation can be measured by a rapid and transient increase in intracellular calcium $[Ca^{2+}]_i$ and pronounced IL-2 production.[39, 40] GABA, the natural endogenous $GABA_AR$ ligand, has been shown to depolarize Jurkat cell plasma membranes, which express $GABA_ARs$ containing a variety of subunits including α4.[21, 41] We determined that GABA had a direct effect on the release of IL-2 from PMA and PHA-stimulated Jurkat cells (Figure 9, A).

GABA at 100 nM significantly reduced secretion of IL-2, but was ineffective at 1 nM. Interestingly, 100 pM XHE-III-74A reduced IL-2 secretion without addition of supplemental GABA, however, GABA is present in media supplemented with 10% bovine serum in addition to GABA endogenously produced by the Jurkat cells.[42, 43] XHE-III-74EE, however, did not reduce IL-2 production under similar conditions (Figure 9A).

We next determined the ability of GABA and GABAergic compounds to modulate increases in intracellular $Ca^{2+}$ in response to PMA and PHA. The highest $[Ca^{2+}]_i$ was observed after 50 seconds following PMA/PHA treatment.[40] The increase in $[Ca^{2+}]_i$ was decreased in a dose dependent manner by GABA and was fully suppressed in the presence of 150 mM GABA (Figure 9B). The $IC_{50}$ of GABA in this assay was 74 ± 3 mM. XHE-III-74A reduced the PMA/PHA-induced increase in $[Ca^{2+}]_i$ at significantly lower concentrations (Figure 9C). The $IC_{50}$ of XHE-III-74A was 210 ± 122 nM. For XHE-III-74EE, we observed merely partial inhibition of PMA/PHA-induced increases in $[Ca^{2+}]_i$ with an $IC_{50}$ value of 24.3 ± 9.8 nM (Figure 9D).

Depolarization of Jurkat cells (human T cell line) at a concentration of 100 μM GABA has been reported.[10] We demonstrated that the effect of GABA on Jurkat cell membrane currents was dose-dependent with an $EC_{50}$ of 3.1 μM (Figure 9E). In the presence of an $EC_3$ concentration of GABA and positive modulator XHE-III-74EE, a significant dose-dependent change of current was observed. A GABA-induced current potentiation of 734% was observed with an XHe-III-74EE $EC_{50}$ of 2.5 μM (Figure 9F). Furthermore, we found that the metabolic product XHE-III-74A potentiated the GABA $EC_3$ current by 808% with an $EC_{50}$

of 0.7 μM (Figure 9F). Thus overall, both $GABA_AR$ modulators have a significant influence on GABA-induced currents in T-cells.

Finally, we investigated the ability of XHE-III-74EE and XHE-III-74A to relax airway smooth muscle, which has previously been reported for the parent compound XHE-III-74 (Figure 10).[18]

In the present study guinea pig smooth muscle rings were contracted *ex vivo* in the presence of substance P which contracts airway smooth muscle by activating Gq-coupled neurokinin receptors.[44] After the establishment of an increase in contractile force, XHE-III-74EE, XHE-III-74A and the parent compound XHe-III-74 (100 μM) induced active relaxation of airway smooth muscle contractile force compared to vehicle treated (0.1% DMSO) rings.

## Discussion

The study expands upon observations that aerosolized XHE-III-74 reduced AHR in house dust mite sensitized mice.[20] While XHE-III-74 is stable in the presence of human microsomes it has a short half-life in the presence of mouse liver microsomes, which impedes investigations in a murine asthma model. Accordingly, the focus of our investigations in this study was a chemically related analog, XHE-III-74EE, which is an α4-selective $GABA_AR$ positive modulator with excellent stability in both human and mouse microsomes.

$GABA_AR$ target verification using immunoblotting showed α1, α2, α4, α5, β3 and γ2 but not α3 $GABA_AR$ subunit expression in whole mouse lung homogenates. In addition, immunohistochemical analysis identified the α4 $GABA_AR$ subunit in airway smooth muscle, epithelium, and chondrocytes. Additional studies are currently ongoing to identify the localization of the other $GABA_AR$ subunits in the mouse lung to identify lung cell types that express functional α4β3γ2 $GABA_ARs$. Additional immune-reactive bands in lung homogenates in comparison to the mouse brain homogenates were observed for the α2, α4, and β3 $GABA_AR$ subunits as a possible result of non-selective binding or cell-specific posttranslational modification of $GABA_AR$ subunits including N-glycosylation.[45]

The distribution and clearance of XHE-III-74EE when administered to mice by i.p. injection was very rapid in both blood and lung. The small and hydrophobic molecule XHE-III-74EE was slowly absorbed in the brain with a significantly later $t_{max}$ in comparison with blood and lung. As a result, impaired sensorimotor coordination was observed at a high dose of 40 mg/kg. Therefore, the studies in the murine asthma model were conducted at lower doses of 10 and 20 mg/kg to avoid these CNS effects. Based on a large AUC value, XHE-III-74EE has good lung exposure, which is partly due to lack of metabolism in this tissue. Overall, the XHE-III-74EE was shown to be more stable compared to rapid conversion to XHE-III-74A *in vivo* in the liver and fast clearance. Thus, the pharmacological exposure of XHE-III-74EE is very limited. The metabolite XHE-III-74A is also rapidly distributed and cleared from blood and lung tissue. XHE-III-74A has minimal BBB penetration and thus no obvious CNS effects and is predominately secreted without metabolism.

The effects of systemic administration of XHE-III-74EE on AHR in the Ova S/C model were moderate and most pronounced during a five day i.p. treatment and seven days with osmotic pump administration. Both XHE-III-74EE and XHE-III-74A caused immediate relaxation of precontracted smooth muscle of trachea rings in an *ex vivo* model. However this effect was less prominent *in vivo* probably due to sub-pharmacological concentrations achieved with most of the dosage regimens. The pharmacokinetic analysis showed that a good exposure of XHE-III-74EE and XHE-III-74A was only achieved for a very short period thus precise timing for acute administration is expected to be crucial. For XHE-III-74A, a single dose regimen showed no changes in specific airway resistance. However, a multi-dose regimen of XHE-III-74EE did cause a reduction in specific airway resistance. The response was more significant for a continuous release using implanted minipumps, which delivered blood concentration of 27.2 ng/mL of XHE-III-74EE compared to a $c_{max}$ of 216 ng/ml with a twice daily i.p. injection. Similar results were observed for the multi-dose administration of anti-inflammatory agent dexamethasone.

XHE-III-74A, and to a lesser extent XHE-III-74EE, showed very pronounced immune suppressive effects on mitogen activated Jurkat cells. This effect is consistent with the acute effect of XHE-III-74A seen in the Ova model. T lymphocyte activation is associated with a transient increase in intracellular $[Ca^{2+}]_i$, which can be triggered with a combination of PMA and PHA.[40] The current model of T cell activation includes the activation of tyrosine kinase and subsequently phospholipase Cy1, which generates diacylglycerol (DAG) and inositol 1,4,5-triphosphate ($IP_3$). $IP_3$ binds to the $IP_3$ receptor of the endoplasmic reticulum (ER) leading to rapid cytoplasmic $Ca^{2+}$ release. This in turn triggers a more continuous process of extracellular $Ca^{2+}$ influx, called store-operated $Ca^{2+}$ entry, mediated by different $Ca^{2+}$ release-activated $Ca^{2+}$ channels in the plasma membrane.[46] This process can be probed with an intracellular $Ca^{2+}$ selective dye that reveals a rapid initial increase of $[Ca^{2+}]_i$ upon PHA/PHA treatment. Herein, we have demonstrated that GABA at a concentration of 30 mM and higher, was able to reduce the $[Ca^{2+}]_i$ levels. At a physiological concentration of around 200-400 nM GABA, however, T lymphocyte activation is unlikely to be reduced by GABA unless $GABA_AR$ positive modulators are present. This effect was again more pronounced for XHE-III-74A than XHE-III-74EE, identifying XHE-III-74A as an immune suppressor. As pointed out, ER calcium release involves mainly enzymatic-based signal transduction in contrast to ion potential-sensitive store-operated $Ca^{2+}$ entry. Although not well understood, the effect of $GABA_AR$ ligands on cellular calcium homeostasis is believed to be mediated by membrane depolarization.[21] T cells have a natural high membrane potential between -50 and -80 mV and a high intracellular chloride concentration (30-40 mM), which upon activation of $GABA_AR$ is assumed to cause an efflux of chloride ions. This is counteracting T cell activation, which has been shown to increase intracellular $Cl^-$ levels[47] to promote store-operated $Ca^{2+}$ entry.[48] GABA at a concentration of 100 μM has been shown to depolarize Jurkat cells,[41] however concentrations as low as 1 μM GABA were found sufficient to evoke current changes in combination with $GABA_AR$ antagonist ER95531.[22] Herein, we report for the first time the $EC_{50}$ for Jurkat cells to be 3.1 μM for GABA. More importantly, small molecules XHE-III-74EE and XHE-III-74A were able to potentiate the current effect of low GABA concentrations in T lymphocytes confirming the presence of $GABA_ARs$ in Jurkat cells.

Elevated calcium levels, observed during T cell activation, activate calcineurin that in turn dephosphorylates and triggers the nuclear localization of NFATc proteins.[49] Once assembled as NFAT transcription complex, genes including IL-2 are transcribed. We have shown that GABA prevented a $[Ca^{2+}]_i$ spike associated with T cell activation in a dose-dependent manner and decreased IL-2 release. At nanomolar concentration, XHE-III-74A exhibited a similar activity.

In the Ova asthma model, we observed a reduction in airway eosinophilia after treatment with XHE-III-74A. Th2 activation *in situ* is mediated by transient calcium signaling that eventually leads to the expression of cytokines including IL-3, IL-5 and IL-13.[50] In asthma, IL-5 and IL-3 are important regulators of eosinophilia in concert with eotaxin. Thus in respect to inflammation, we were able to show that GABAergic compound XHE-III-74A has *in vitro* and *in vivo* anti-inflammatory properties.

The GABAergic system has been implicated in the overproduction of mucus in Ova S/C model.[26] Thus it would be predicted that non-selective GABAeric agents, especially those activating the α2 containing $GABA_AR$, would increase mucus production. In contrast, α4-selective compounds evaluated in this study did not increase mucus production.

Data from this initial study with XHE-III-74EE and XHE-III-74A support the use of α4-selective $GABA_AR$ ligands as novel drug candidates for asthma. The symptoms of asthma in a murine model of asthma that include AHR, eosinophilia, inflammation, and mucus overproduction were partially alleviated. From the initial compounds studied herein, a series of related subunit selective $GABA_AR$ ligands are being developed to improve pharmacokinetic properties. It is expected that the resulting compounds have improved target tissue drug exposure that will improve dosing and disease efficacy measures in murine asthma models. We will also use these compounds as probes to better understand the role of the α4 subunit containing GABAergic system during the immune response.

## Supplementary Material

Refer to Web version on PubMed Central for supplementary material.

## Acknowledgments

We thank Dr. Beryl R. Forman and Jennifer L. Nemke (Animal Facility at UWM) for their guidance and support.

**Funding Sources**: This work was supported by the University of Wisconsin-Milwaukee, the National Institutes of Health R03DA031090 (LAA), R01NS076517 (JMC, LAA), R01HL118561 (JMC, LAA, CWE, DCS), R01MH096463 (JMC, LAA), R01GM065281 (CWE, GTY, JMC) and R01HL122340 (CWE) as well as the University of Wisconsin Milwaukee Research Foundation (Catalyst grant), the Lynde and Harry Bradley Foundation, the Richard and Ethel Herzfeld Foundation, the Stony Wold-Herbert Fund (GTY), the Foundation for Anesthesia Education and Research (GTY), and the Austrian Science Fund I 2306-B27 (M.T. and M.E.) and W1232 (M.E.).

## References

1. Trends in asthma morbidity and mortality. American Lung Association Epidemiology & Statistics Unit Research and Program Services. Washington, DC: 2012.

2. Pascual RM, Peters SP. Airway remodeling contributes to the progressive loss of lung function in asthma: an overview. J Allergy Clin Immunol. 2005; 116(3):477–86. quiz 487. [PubMed: 16159612]

3. Cates CJ, Cates MJ. Regular treatment with salmeterol for chronic asthma: serious adverse events. Cochrane Database Syst Rev. 2008; (3):CD006363. [PubMed: 18646149]

4. Cates CJ, Cates MJ. Regular treatment with formoterol for chronic asthma: serious adverse events. Cochrane Database Syst Rev. 2012; 4:CD006923. [PubMed: 22513944]

5. Dahl R. Systemic side effects of inhaled corticosteroids in patients with asthma. Respir Med. 2006; 100(8):1307–17. [PubMed: 16412623]

6. Kelly HW, Sternberg AL, Lescher R, Fuhlbrigge AL, Williams P, Zeiger RS, Raissy HH, Van Natta ML, Tonascia J, Strunk RC, Group CR. Effect of inhaled glucocorticoids in childhood on adult height. N Engl J Med. 2012; 367(10):904–12. [PubMed: 22938716]

7. Bhat R, Axtell R, Mitra A, Miranda M, Lock C, Tsien RW, Steinman L. Inhibitory role for GABA in autoimmune inflammation. Proceedings of the National Academy of Sciences of the United States of America. 2010; 107(6):2580–5. [PubMed: 20133656]

8. Mizuta K, Xu D, Pan Y, Comas G, Sonett JR, Zhang Y, Panettieri RA Jr, Yang J, Emala CW Sr. GABAA receptors are expressed and facilitate relaxation in airway smooth muscle. Am J Physiol Lung Cell Mol Physiol. 2008; 294(6):L1206–16. [PubMed: 18408071]

9. Prud'homme GJ, Glinka Y, Wang Q. Immunological GABAergic interactions and therapeutic applications in autoimmune diseases. Autoimmun Rev. 2015; 14(11):1048–56. [PubMed: 26226414]

10. Mortensen M, Patel B, Smart TG. GABA Potency at GABA(A) Receptors Found in Synaptic and Extrasynaptic Zones. Front Cell Neurosci. 2011; 6:1. [PubMed: 22319471]

11. Olsen RW, Sieghart W. International Union of Pharmacology. LXX. Subtypes of gamma-aminobutyric acid(A) receptors: classification on the basis of subunit composition, pharmacology, and function. Update. Pharmacol Rev. 2008; 60(3):243–60. [PubMed: 18790874]

12. Sieghart W, Sperk G. Subunit composition, distribution and function of GABA(A) receptor subtypes. Curr Top Med Chem. 2002; 2(8):795–816. [PubMed: 12171572]

13. Clayton T, Poe MM, Rallapalli S, Biawat P, Savic MM, Rowlett JK, Gallos G, Emala CW, Kaczorowski CC, Stafford DC, Arnold LA, Cook JM. A Review of the Updated Pharmacophore for the Alpha 5 GABA(A) Benzodiazepine Receptor Model. International journal of medicinal chemistry. 2015; 2015:430248. [PubMed: 26682068]

14. Botta P, Demmou L, Kasugai Y, Markovic M, Xu C, Fadok JP, Lu T, Poe MM, Xu L, Cook JM, Rudolph U, Sah P, Ferraguti F, Luthi A. Regulating anxiety with extrasynaptic inhibition. Nature neuroscience. 2015; 18(10):1493–500. [PubMed: 26322928]

15. Dias R, Sheppard WF, Fradley RL, Garrett EM, Stanley JL, Tye SJ, Goodacre S, Lincoln RJ, Cook SM, Conley R, Hallett D, Humphries AC, Thompson SA, Wafford KA, Street LJ, Castro JL, Whiting PJ, Rosahl TW, Atack JR, McKernan RM, Dawson GR, Reynolds DS. Evidence for a significant role of alpha 3-containing GABAA receptors in mediating the anxiolytic effects of benzodiazepines. J Neurosci. 2005; 25(46):10682–8. [PubMed: 16291941]

16. Jacob TC, Moss SJ, Jurd R. GABA(A) receptor trafficking and its role in the dynamic modulation of neuronal inhibition. Nat Rev Neurosci. 2008; 9(5):331–43. [PubMed: 18382465]

17. Rudolph U, Crestani F, Benke D, Brunig I, Benson JA, Fritschy JM, Martin JR, Bluethmann H, Mohler H. Benzodiazepine actions mediated by specific gamma-aminobutyric acid(A) receptor subtypes. Nature. 1999; 401(6755):796–800. [PubMed: 10548105]

18. Yocum GT, Gallos G, Zhang Y, Jahan R, Stephen MR, Varagic Z, Puthenkalam R, Ernst M, Cook JM, Emala CW. Targeting the gamma-Aminobutyric Acid A Receptor alpha4 Subunit in Airway Smooth Muscle to Alleviate Bronchoconstriction. Am J Respir Cell Mol Biol. 2016; 54(4):546–53. [PubMed: 26405827]

19. Gallos G, Yocum GT, Siviski ME, Yim PD, Fu XW, Poe MM, Cook JM, Harrison N, Perez-Zoghbi J, Emala CW Sr. Selective targeting of the alpha5-subunit of GABAA receptors relaxes airway smooth muscle and inhibits cellular calcium handling. Am J Physiol Lung Cell Mol Physiol. 2015; 308(9):L931–42. [PubMed: 25659897]

20. Gallos G, Yim P, Chang S, Zhang Y, Xu D, Cook JM, Gerthoffer WT, Emala CW Sr. Targeting the restricted alpha-subunit repertoire of airway smooth muscle GABAA receptors augments airway smooth muscle relaxation. Am J Physiol Lung Cell Mol Physiol. 2012; 302(2):L248–56. [PubMed: 21949156]
21. Alam S, Laughton DL, Walding A, Wolstenholme AJ. Human peripheral blood mononuclear cells express GABAA receptor subunits. Molecular immunology. 2006; 43(9):1432–42. [PubMed: 16213022]
22. Bjurstrom H, Wang J, Ericsson I, Bengtsson M, Liu Y, Kurnar-Mendu S, Issazadeh-Navikas S, Birnir B. GABA, a natural immunomodulator of T lymphocytes. J Neuroimmunol. 2008; 205(1-2): 44–50. [PubMed: 18954912]
23. Wheeler DW, Thompson AJ, Corletto F, Reckless J, Loke JCT, Lapaque N, Grant AJ, Mastroeni P, Grainger DJ, Padgett CL, O'Brien JA, Miller NGA, Trowsdale J, Lummis SCR, Menon DK, Beech JS. Anaesthetic Impairment of Immune Function Is Mediated via GABA(A) Receptors. PloS one. 2011; 6(2)
24. Reyes-Garcia MG, Hernandez-Hernandez F, Hernandez-Tellez B, Garcia-Tamayo F. GABA (A) receptor subunits RNA expression in mice peritoneal macrophages modulate their IL-6/IL-12 production. J Neuroimmunol. 2007; 188(1-2):64–8. [PubMed: 17599468]
25. Munroe ME, Businga TR, Kline JN, Bishop GA. Anti-inflammatory effects of the neurotransmitter agonist Honokiol in a mouse model of allergic asthma. J Immunol. 2010; 185(9):5586–97. [PubMed: 20889543]
26. Xiang YY, Wang S, Liu M, Hirota JA, Li J, Ju W, Fan Y, Kelly MM, Ye B, Orser B, O'Byrne PM, Inman MD, Yang X, Lu WY. A GABAergic system in airway epithelium is essential for mucus overproduction in asthma. Nat Med. 2007; 13(7):862–7. [PubMed: 17589520]
27. Ramerstorfer J, Furtmuller R, Vogel E, Huck S, Sieghart W. The point mutation gamma 2F77I changes the potency and efficacy of benzodiazepine site ligands in different GABA(A) receptor subtypes. European journal of pharmacology. 2010; 636(1-3):18–27. [PubMed: 20303942]
28. Li XY, Ma CR, He XH, Yu JM, Han DM, Zhang CC, Atack JR, Cook JM. Studies in search of diazepam-insensitive subtype selective agents for GABA(A)/Bz receptors. Med Chem Res. 2002; 11(9):504–537.
29. Nguyen LP, Omoluabi O, Parra S, Frieske JM, Clement C, Ammar-Aouchiche Z, Ho SB, Ehre C, Kesimer M, Knoll BJ, Tuvim MJ, Dickey BF, Bond RA. Chronic exposure to beta-blockers attenuates inflammation and mucin content in a murine asthma model. Am J Respir Cell Mol Biol. 2008; 38(3):256–62. [PubMed: 18096872]
30. Glaab T, Taube C, Braun A, Mitzner W. Invasive and noninvasive methods for studying pulmonary function in mice. Respiratory research. 2007; 8:63. [PubMed: 17868442]
31. Evans CM, Williams OW, Tuvim MJ, Nigam R, Mixides GP, Blackburn MR, DeMayo FJ, Burns AR, Smith C, Reynolds SD, Stripp BR, Dickey BF. Mucin is produced by clara cells in the proximal airways of antigen-challenged mice. Am J Respir Cell Mol Biol. 2004; 31(4):382–94. [PubMed: 15191915]
32. Piccotti L, Dickey BF, Evans CM. Assessment of intracellular mucin content in vivo. Methods in molecular biology. 2012; 842:279–95. [PubMed: 22259143]
33. Nguyen LP, Lin R, Parra S, Omoluabi O, Hanania NA, Tuvim MJ, Knoll BJ, Dickey BF, Bond RA. Beta2-adrenoceptor signaling is required for the development of an asthma phenotype in a murine model. Proceedings of the National Academy of Sciences of the United States of America. 2009; 106(7):2435–40. [PubMed: 19171883]
34. Henderson WR Jr, Lewis DB, Albert RK, Zhang Y, Lamm WJ, Chiang GK, Jones F, Eriksen P, Tien YT, Jonas M, Chi EY. The importance of leukotrienes in airway inflammation in a mouse model of asthma. The Journal of experimental medicine. 1996; 184(4):1483–94. [PubMed: 8879219]
35. Mhatre MC, Pena G, Sieghart W, Ticku MK. Antibodies specific for GABAA receptor alpha subunits reveal that chronic alcohol treatment down-regulates alpha-subunit expression in rat brain regions. Journal of neurochemistry. 1993; 61(5):1620–5. [PubMed: 8228981]

36. Jin N, Narasaraju T, Kolliputi N, Chen J, Liu L. Differential expression of GABAA receptor pi subunit in cultured rat alveolar epithelial cells. Cell and tissue research. 2005; 321(2):173–83. [PubMed: 15912403]
37. Jacques P, Perret P, Bouchet MJ, Foucaud B, Goeldner M, Benke D. Irreversible site-directed labeling of the 4-aminobutyrate binding site by tritiated meta-sulfonate benzene diazonium. Contribution of a nucleophilic amino acid residue of the alpha1 subunit. European journal of biochemistry / FEBS. 1999; 265(1):189–94. [PubMed: 10491173]
38. Eum SY, Maghni K, Hamid Q, Eidelman DH, Campbell H, Isogai S, Martin JG. Inhibition of allergic airways inflammation and airway hyperresponsiveness in mice by dexamethasone: role of eosinophils, IL-5, eotaxin, and IL-13. J Allergy Clin Immunol. 2003; 111(5):1049–61. [PubMed: 12743570]
39. Pawelec G, Borowitz A, Krammer PH, Wernet P. Constitutive interleukin 2 production by the JURKAT human leukemic T cell line. European journal of immunology. 1982; 12(5):387–92. [PubMed: 6980126]
40. Weiss A, Imboden J, Shoback D, Stobo J. Role of T3 surface molecules in human T-cell activation: T3-dependent activation results in an increase in cytoplasmic free calcium. Proceedings of the National Academy of Sciences of the United States of America. 1984; 81(13):4169–73. [PubMed: 6234599]
41. Dionisio L, Arias V, Bouzat C, Esandi Mdel C. GABAA receptor plasticity in Jurkat T cells. Biochimie. 2013; 95(12):2376–84. [PubMed: 24012548]
42. Minuk GY, Winder A, Burgess ED, Sarjeant EJ. Serum gamma-aminobutyric acid (GABA) levels in patients with hepatic encephalopathy. Hepato-gastroenterology. 1985; 32(4):171–4. [PubMed: 4054811]
43. Nigam R, El-Nour H, Amatya B, Nordlind K. GABA and GABA(A) receptor expression on immune cells in psoriasis: a pathophysiological role. Archives of dermatological research. 2010; 302(7):507–15. [PubMed: 20455067]
44. Garcia-Recio S, Gascon P. Biological and Pharmacological Aspects of the NK1-Receptor. BioMed research international. 2015; 2015:495704. [PubMed: 26421291]
45. Mueller TM, Haroutunian V, Meador-Woodruff JH. N-Glycosylation of GABA(A) Receptor Subunits is Altered in Schizophrenia. Neuropsychopharmacol. 2014; 39(3):528–537.
46. Nohara LL, Stanwood SR, Omilusik KD, Jefferies WA. Tweeters, Woofers and Horns: The Complex Orchestration of Calcium Currents in T Lymphocytes. Frontiers in immunology. 2015; 6:234. [PubMed: 26052328]
47. Lai ZF, Chen YZ, Nishi K. Modulation of intracellular Cl- homeostasis by lectin-stimulation in Jurkat T lymphocytes. European journal of pharmacology. 2003; 482(1-3):1–8. [PubMed: 14659998]
48. Kerschbaum HH, Negulescu PA, Cahalan MD. Ion channels, Ca2+ signaling, and reporter gene expression in antigen-specific mouse T cells. J Immunol. 1997; 159(4):1628–38. [PubMed: 9257822]
49. Crabtree GR, Olson EN. NFAT signaling: choreographing the social lives of cells. Cell. 2002; 109 Suppl:S67–79. [PubMed: 11983154]
50. Asquith KL, Ramshaw HS, Hansbro PM, Beagley KW, Lopez AF, Foster PS. The IL-3/IL-5/GM-CSF common receptor plays a pivotal role in the regulation of Th2 immunity and allergic airway inflammation. J Immunol. 2008; 180(2):1199–206. [PubMed: 18178860]

## Abbreviations

| | |
|---|---|
| **$GABA_AR$** | $GABA_A$ receptor |
| **ASM** | airway smooth muscle |
| **LPS** | lipopolysaccharide |
| **BBB** | blood brain barrier |

| | |
|---|---|
| **PAFS** | periodic acid fluorescent Schiff's stain |
| **BALF** | bronchoalveolar lavage fluid |
| **PHA** | phytohemagglutinin |
| **PMA** | phorbol myristate acetate |
| **Il-2** | interleukin 2 |
| **DMSO** | dimethyl sulfoxide |
| **AUC** | area under the curve |
| **CNS** | central nervous system |
| **DAG** | diacetylglycerol |
| **$IP_3$** | inositol 1,4,5-triposphate |
| **ER** | endoplasmic reticulum |

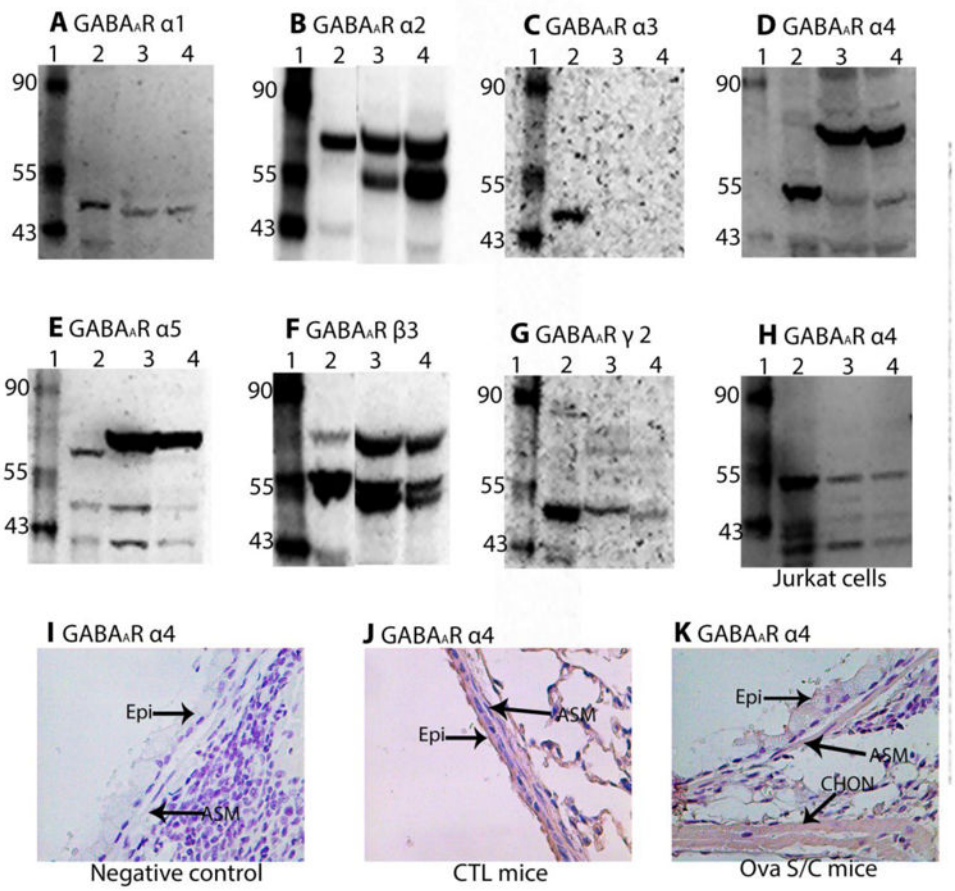


**Figure 1. Immunoblot analysis and immunohistochemical detection of GABAA receptor subunits**

Representative immunoblot (A-G) from mouse lung homogenates, (H) cultured Jurkat cells, and (I-K) immunohistochemical images from control and Ova S/C BALB/c mouse lung. Immunoblot studies were performed using antibodies to $GABA_A$ receptor subunits in 70 μg of membrane protein harvested from whole lungs. Lane 1: molecular weight marker (kDa); lane 2: positive controls (α1, α3, α5, β3: mouse brain extract, α4: H4 cell lysate, α2 and γ2: mouse cerebellum extract); lane 3: membrane protein extracted from Ova S/C Balb/c mice or Jurkat; lane 4: membrane protein extracted from control Balb/c mice or Jurkat. Immunohistochemical staining was done using formalin fixed and paraffin embedded mouse lung sections. (Epi; airway epithelium, ASM; airway smooth muscles, CHON; chondrocytes.

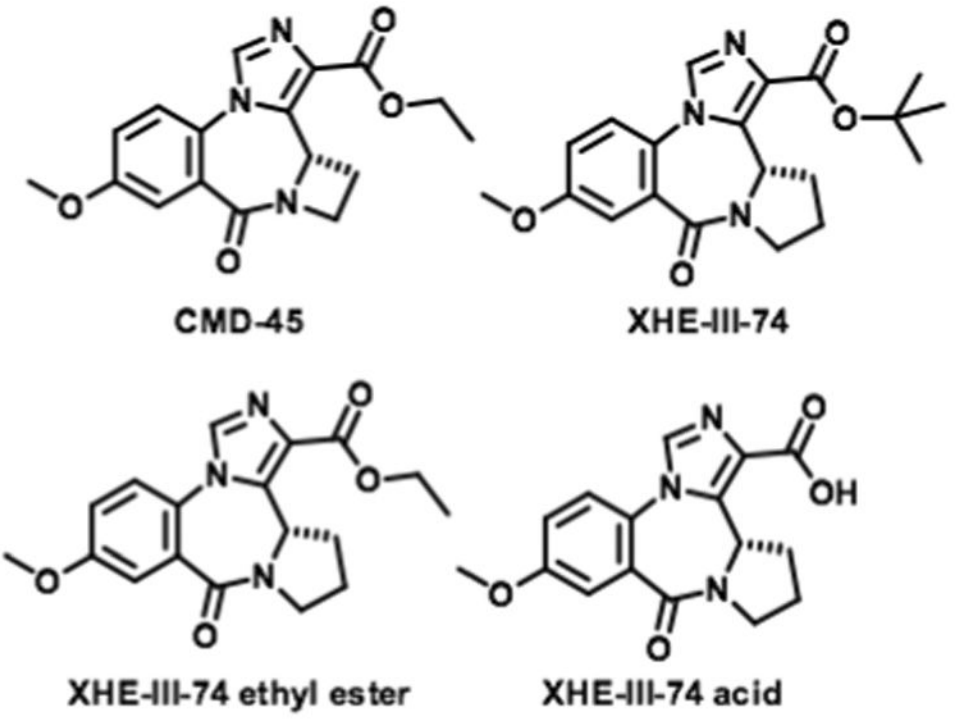


**Figure 2. Chemical structure of CMD-45, XHE-III-74, XHE-III-74EE and XHE-III-74A**

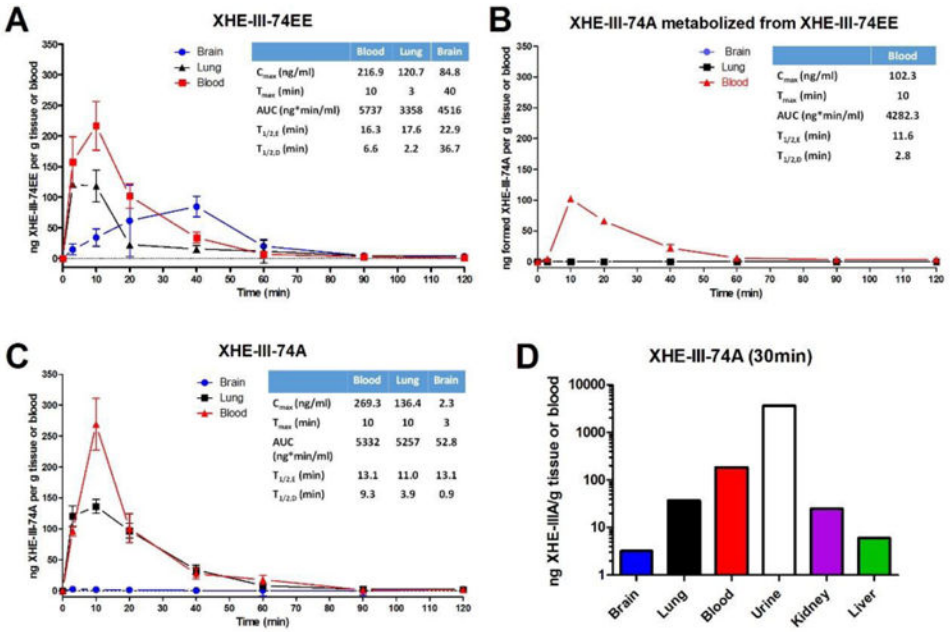


**Figure 3. Pharmacokinetic profile of XHE-III-74 EE and XHE-III-74A in mice brain, lung and blood (N = 3): A)**

Time dependent distribution of XHE-III-74EE (5 mg/kg, i.p.); **B**) Time dependent distribution of metabolite XHE-III-74A given as XHE-III-74EE (5 mg/kg, i.p.), **C**) Time dependent distribution of XHE-III-74A (5 mg/kg, i.p.); **D**) Distribution of XHE-III-74A (5 mg/kg, i.p.) at 30 minutes in different tissue and fluids (N = 1).

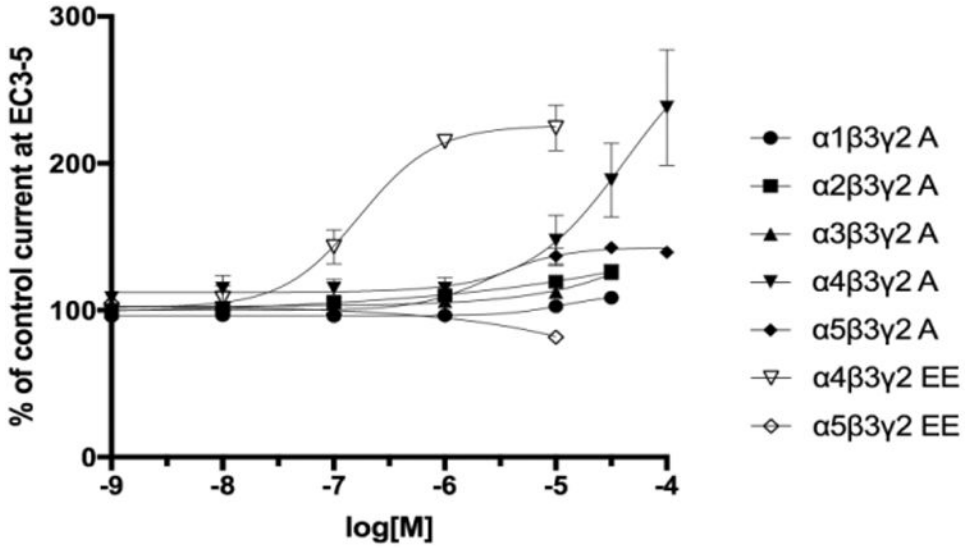


**Figure 4. GABAA receptor subtype selectivity**

Dose dependent modulation of GABA ($EC_{3-5}$ concentration) elicited currents by XHE-III-74A (A) and XHE-III-74EE (EE) on Xenopus oocytes expressing $GABA_A$ receptor subtypes α1β3γ2, α2β3γ2, α3β3γ2, α4β3γ2 and α5β3γ2. Data points represent means ± SEM from 2-8 oocytes from 2 batches, normalized to control currents (100%) in the absence of compound. XHE-III-74EE modulation of a set of $GABA_AR$ subtypes has been published previously,[27] and only α4β3γ2 and α5β3γ2 are shown here for comparison. XHE-III-74EE modulation of α5β3γ2 $GABA_AR$ was measured at GABA EC20.

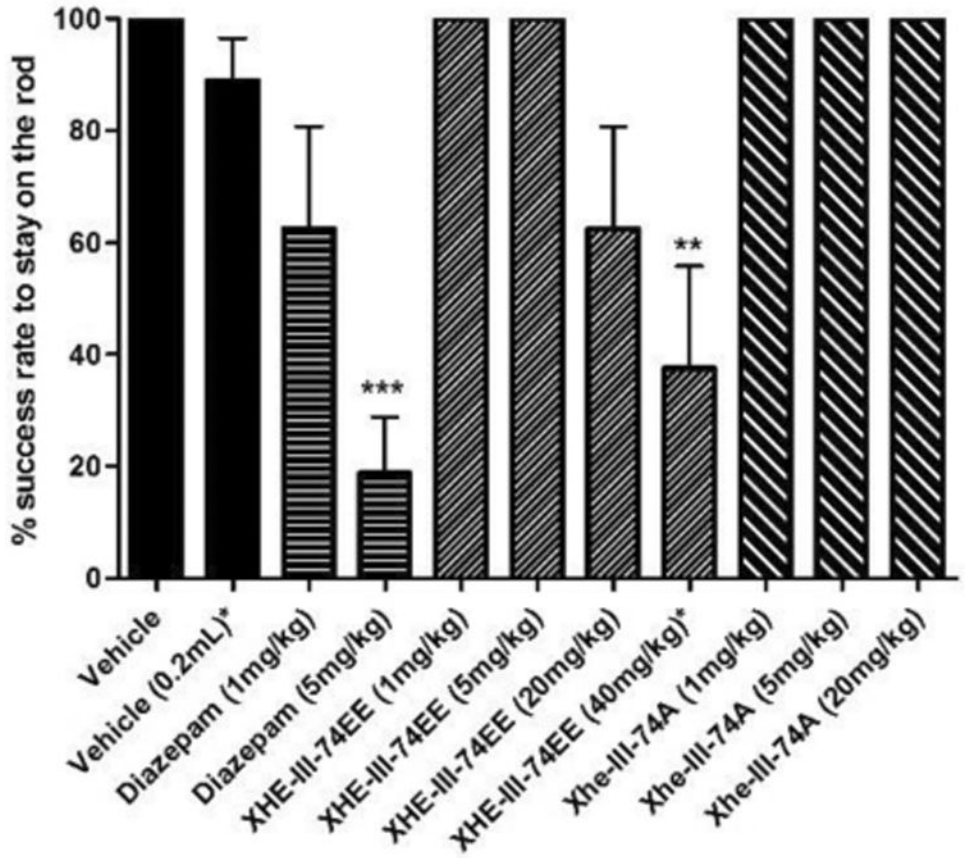


**Figure 5. Effect of XHE-III-74EE and XHE-III-74A on sensorimotor coordination**

Balb/c mice were tested on a rotarod at 15 rpm for three minutes. Mice received a single i.p. injection of test compound or control compound. A fail was assigned to a mouse that fell from the rotarod prior to three minutes. % success rate is expressed as mean ± SEM ($N$ = 8). **, *** indicates $p<0.01$, $p<0.001$ significance compared to vehicle treated mice.

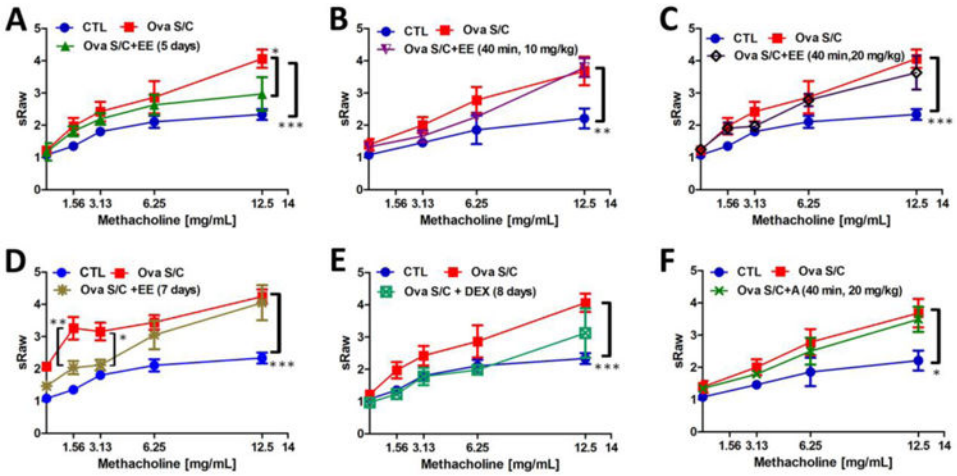


**Figure 6. Effect of XHE-III-74EE (EE) and XHE-III-74A (A) on airway hyperresponsiveness**

Specific airway resistance (sRaw) to increasing doses of methacholine measured by DSI's Buxco® FinePointe non-invasive airway mechanics instrument. Balb/c mice were administered (A) XHE-III-74EE, two 20 mg/kg i.p. injections daily for 5 days (B) XHE-III-74EE, single i.p. injection 10 mg/kg 40 minutes prior to analysis; (C) XHE-III-74EE, single i.p. injection 20 mg/kg 40 minutes prior to analysis; (D) XHE-III-74EE via osmotic pump, 20 mg/kg daily for 7 days; (E) DEX, single 4 mg/kg i.p. injection daily for 8 days and (F) XHE-III-74A, single i.p. injection 20 mg/kg 40 minutes prior to analysis. Data represent mean ± SEM from 4-7 mice in each group. *, **, *** indicates $p<0.05$, $p<0.01$, $p<0.001$ significance compared to vehicle treated Ova S/C Balb/c mice.

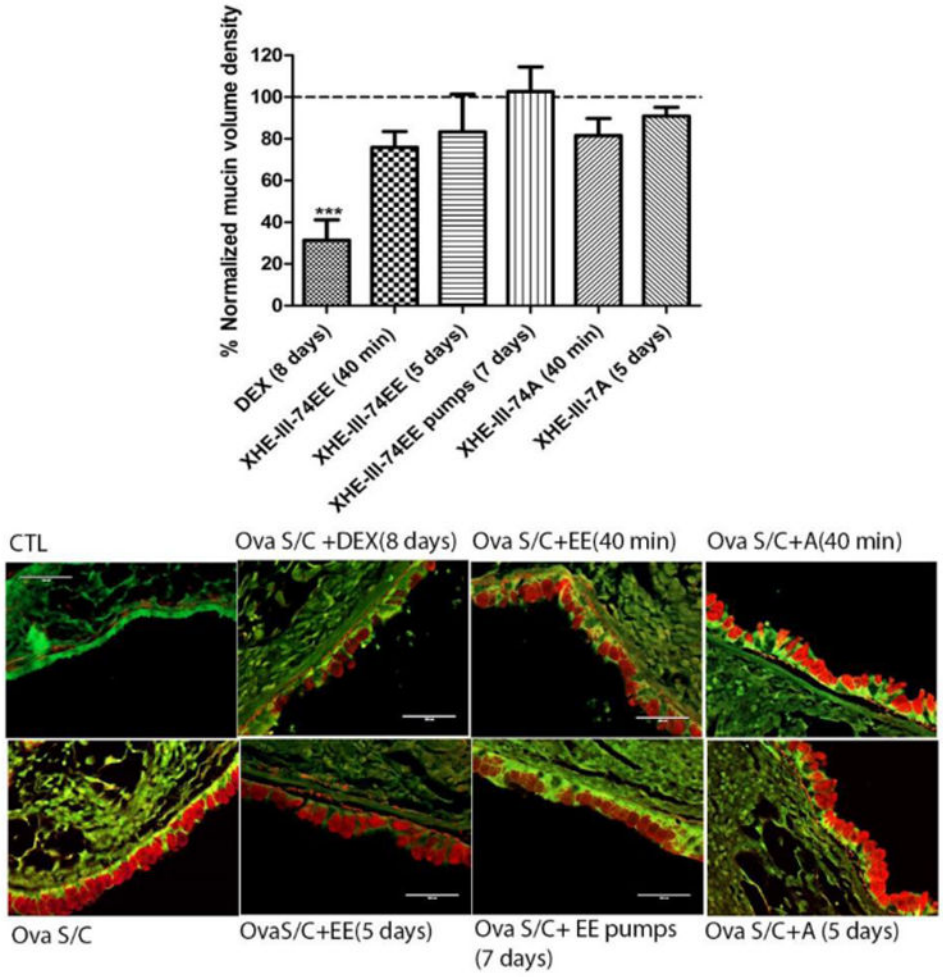


**Figure 7. Effect of XHE-III-74EE (EE) and XHE-III-74A on mucin production**

(A) Morphometric quantification of mucin volume density and (B) representative images of mucin (red) in the airway epithelium (green) with periodic acid fluorescent schiff's stain. Balb/c mice were administered once daily 4 mg/kg i.p. DEX (dexamethasone) injections for 8 days, a single 20 mg/kg i.p. injection of XHE-III-74EE 40 minutes prior to analysis, two XHE-III-74 EE 20 mg/kg i.p. injections daily for 5 days, 20 mg/kg XHE-III-74EE for 7 days via osmotic pump, XHE-III-74 EE single 20 mg/kg i.p. injection 40 minutes prior to analysis, or two XHE-III-74A 20 mg/kg i.p. injection daily for 5 days. Data represent % normalized mucin volume density relative to CTL and Ova S/C Balb/c mice from 5-7 mice in each group. ** indicates $p<0.01$ significance compared to vehicle treated Ova S/C Balb/c mice. Scale bar represents 100 μm.

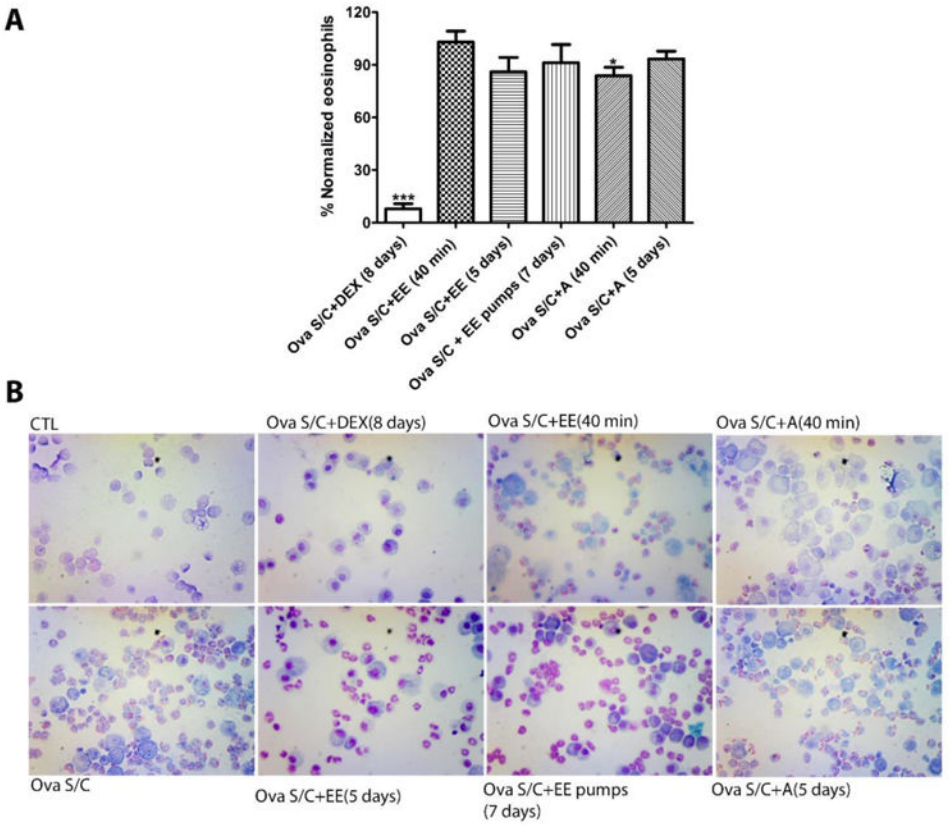


**Figure 8. Effect of XHE-III-74EE (EE) and XHE-III-74A (A) on airway eosinophilia**

(A) Quantification of airway eosinophilia and (B) representative images of Wright Giemsa stained slides. Balb/c mice were administered single 4 mg/kg i.p. DEX (dexamethasone) injection daily for 8 days, XHE-III-74 EE single 20 mg/kg i.p. injection 40 minutes prior to analysis, two XHE-III-74 EE 20 mg/kg i.p. injections daily for 5 days, 20 mg/kg XHE-III-74 EE via osmotic pump for 7 days, XHE-III-74 EE single 20 mg/kg i.p. injection 40 minutes prior to analysis, and two XHE-III-74A 20 mg/kg i.p. injections daily for 5 days. Data represent % normalized eosinophils relative to CTL (negative control) and Ova S/C Balb/c mice (positive control) from 5-7 mice in each group. * and *** indicates $p<0.05$ and $p<0.001$ significance compared to vehicle treated Ova S/C Balb/c mice.

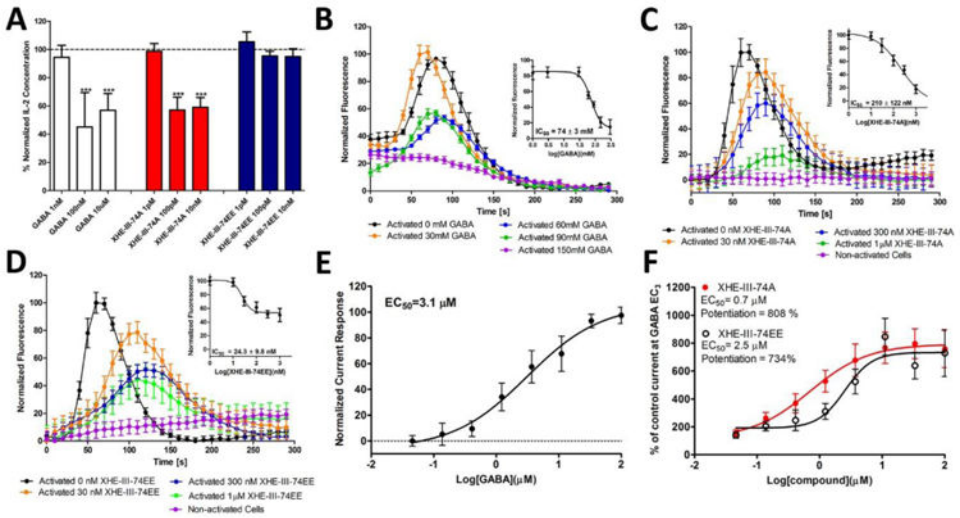


**Figure 9. Modulation of immune response**

$GABA_AR$ ligands inhibit intracellular calcium spike and increased IL-2 production in PMA/PHA stimulated Jurkat cells. A) IL-2 in the presence of different concentrations of GABA, XHE-74EE and XHE-74A; B, C, D) decrease of $[Ca^{2+}]_i$ concentration in Jurkat cells measured with a cell-permeable fluorescence probe Fluo-4 in the presence of different concentrations GABA, XHE-III-74A and XHE-III-74EE; E) Patch-clamped change of Jurkat current response in the presence of GABA; F) Patch clamped change of Jurkat current response in the presence of 300 nM GABA and XHE-III-74A and XHE-III-74EE. *** indicates $p<0.001$ significance compared to vehicle treated activated Jurkat cells.

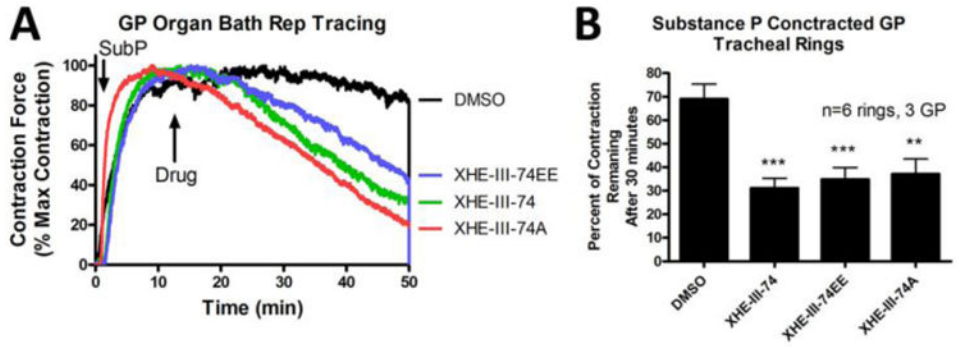


**Figure 10. Muscle force measurements in guinea pig tracheal rings**

A) Time-dependent change of muscle contraction in the presence of substance P and GABAergic compounds; B) Force remaining 30 minutes after drug addition is shown. Tracheal rings were contracted with 1μM substance P and at the peak of muscle contraction 100 μM (in 0.1% DMSO) was added and the percent of remaining force was measured at 30 min. *** $p < 0.001$, ** $p < 0.01$ compared to vehicle, n=6 rings from 3 guinea pigs (GP).

**Table 1**

**In vitro metabolic stability of XHE-III-74, XHE-III-74EE and XHE-III-74A**

| | XHE-III-74 | XHE-III-74EE | XHE-III-74A |
|---|---|---|---|
| human liver microsomes % remaining after 1 hour | 92.1 ± 1.0 | 99.2 ± 0.15 | 56.5 ± 0.6 |
| Mouse liver microsomes % remaining after 1 hour | 24.1 ± 0.7 | 86.3 ± 0.3 | 51.3 ± 0.4 |
| human S9 fraction % remaining after 1 hour | - | 95.6 ± 0.3 | 82.5 ± 0.2 |
| Mouse S9 fraction % remaining after 1 hour | - | 98.4 ± 0.4 | 64.2 ± 0.2 |
| Mouse plasma | - | 92.6 ± 0.2 | 91.9 ± 0.4 |

* Half-life, intrinsic clearance and metabolic rates calculated for each experiment are presented in the Supporting Information.